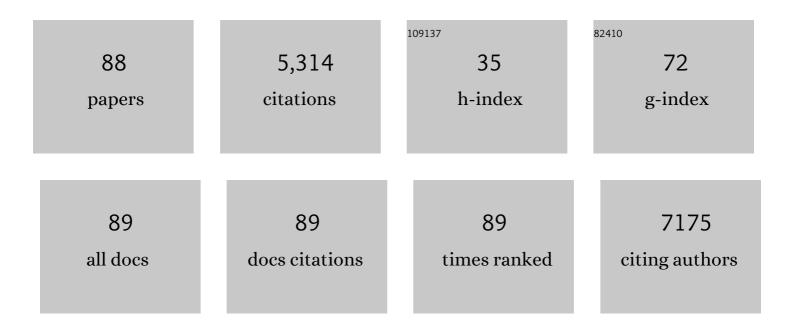
List of Publications by Year in descending order

Source: https://exaly.com/author-pdf/2756979/publications.pdf Version: 2024-02-01



#	Article	IF	CITATIONS
1	CH ₃ NH ₃ Sn _{<i>x</i>} Pb _(1–<i>x</i>) I ₃ Perovskite Solar Cells Covering up to 1060 nm. Journal of Physical Chemistry Letters, 2014, 5, 1004-1011.	2.1	852
2	Highly Luminescent Phase-Stable CsPbI ₃ Perovskite Quantum Dots Achieving Near 100% Absolute Photoluminescence Quantum Yield. ACS Nano, 2017, 11, 10373-10383.	7.3	748
3	Colloidal Synthesis of Air-Stable Alloyed CsSn _{1–<i>x</i>} Pb _{<i>x</i>} I ₃ Perovskite Nanocrystals for Use in Solar Cells. Journal of the American Chemical Society, 2017, 139, 16708-16719.	6.6	314
4	Mixed Sn–Ge Perovskite for Enhanced Perovskite Solar Cell Performance in Air. Journal of Physical Chemistry Letters, 2018, 9, 1682-1688.	2.1	206
5	High Electrical Conductivity 2D MXene Serves as Additive of Perovskite for Efficient Solar Cells. Small, 2018, 14, e1802738.	5.2	193
6	All-Solid Perovskite Solar Cells with HOCO-R-NH ₃ ⁺ I [–] Anchor-Group Inserted between Porous Titania and Perovskite. Journal of Physical Chemistry C, 2014, 118, 16651-16659.	1.5	191
7	Allâ€Inorganic CsPb _{1â^'<i>x</i>} Ge _{<i>x</i>} I ₂ Br Perovskite with Enhanced Phase Stability and Photovoltaic Performance. Angewandte Chemie - International Edition, 2018, 57, 12745-12749.	7.2	157
8	Achievable high <i>V</i> _{oc} of carbon based all-inorganic CsPbIBr ₂ perovskite solar cells through interface engineering. Journal of Materials Chemistry A, 2019, 7, 1227-1232.	5.2	115
9	Highly Efficient 17.6% Tin–Lead Mixed Perovskite Solar Cells Realized through Spike Structure. Nano Letters, 2018, 18, 3600-3607.	4.5	114
10	Strain Relaxation and Light Management in Tin–Lead Perovskite Solar Cells to Achieve High Efficiencies. ACS Energy Letters, 2019, 4, 1991-1998.	8.8	114
11	Gel ₂ Additive for High Optoelectronic Quality CsPbl ₃ Quantum Dots and Their Application in Photovoltaic Devices. Chemistry of Materials, 2019, 31, 798-807.	3.2	112
12	Effect of the conduction band offset on interfacial recombination behavior of the planar perovskite solar cells. Nano Energy, 2018, 53, 17-26.	8.2	110
13	Niobium Incorporation into CsPbl ₂ Br for Stable and Efficient All-Inorganic Perovskite Solar Cells. ACS Applied Materials & Interfaces, 2019, 11, 19994-20003.	4.0	106
14	Role of GeI2 and SnF2 additives for SnGe perovskite solar cells. Nano Energy, 2019, 58, 130-137.	8.2	104
15	Facile Synthesis and Characterization of Sulfur Doped Low Bandgap Bismuth Based Perovskites by Soluble Precursor Route. Chemistry of Materials, 2016, 28, 6436-6440.	3.2	87
16	Optical absorption, charge separation and recombination dynamics in Sn/Pb cocktail perovskite solar cells and their relationships to photovoltaic performances. Journal of Materials Chemistry A, 2015, 3, 9308-9316.	5.2	85
17	Efficiency enhancement by changing perovskite crystal phase and adding a charge extraction interlayer in organic amine free-perovskite solar cells based on cesium. Solar Energy Materials and Solar Cells, 2016, 144, 532-536.	3.0	79
18	Ultrafast Electron Injection from Photoexcited Perovskite CsPbI ₃ QDs into TiO ₂ Nanoparticles with Injection Efficiency near 99%. Journal of Physical Chemistry Letters, 2018, 9, 294-297.	2.1	75

#	Article	IF	CITATIONS
19	Enhanced Crystallization by Methanol Additive in Antisolvent for Achieving Highâ€Quality MAPbl ₃ Perovskite Films in Humid Atmosphere. ChemSusChem, 2018, 11, 2348-2357.	3.6	70
20	Passivation of Grain Boundary by Squaraine Zwitterions for Defect Passivation and Efficient Perovskite Solar Cells. ACS Applied Materials & Interfaces, 2019, 11, 10012-10020.	4.0	70
21	Solution-processed intermediate-band solar cells with lead sulfide quantum dots and lead halide perovskites. Nature Communications, 2019, 10, 43.	5.8	70
22	Tunable Open Circuit Voltage by Engineering Inorganic Cesium Lead Bromide/Iodide Perovskite Solar Cells. Scientific Reports, 2018, 8, 2482.	1.6	62
23	Interfacial Sulfur Functionalization Anchoring SnO ₂ and CH ₃ NH ₃ PbI ₃ for Enhanced Stability and Trap Passivation in Perovskite Solar Cells. ChemSusChem, 2018, 11, 3941-3948.	3.6	58
24	Slow hot carrier cooling in cesium lead iodide perovskites. Applied Physics Letters, 2017, 111, .	1.5	56
25	Effects of Temperature on Electrochemical Properties of Bismuth Oxide/Manganese Oxide Pseudocapacitor. Industrial & Engineering Chemistry Research, 2018, 57, 2146-2154.	1.8	54
26	Direct observation of dramatically enhanced hole formation in a perovskite-solar-cell material spiro-OMeTAD by Li-TFSI doping. Applied Physics Letters, 2017, 110, .	1.5	53
27	Cesium Lead Halide Inorganic-Based Perovskite-Sensitized Solar Cell for Photo-Supercapacitor Application under High Humidity Condition. ACS Applied Energy Materials, 2018, 1, 692-699.	2.5	52
28	Improved Reproducibility and Intercalation Control of Efficient Planar Inorganic Perovskite Solar Cells by Simple Alternate Vacuum Deposition of PbI ₂ and CsI. ACS Omega, 2017, 2, 4464-4469.	1.6	49
29	The Role of Lanthanum in a Nickel Oxideâ€Based Inverted Perovskite Solar Cell for Efficiency and Stability Improvement. ChemSusChem, 2019, 12, 518-526.	3.6	49
30	Air Stable PbSe Colloidal Quantum Dot Heterojunction Solar Cells: Ligand-Dependent Exciton Dissociation, Recombination, Photovoltaic Property, and Stability. Journal of Physical Chemistry C, 2016, 120, 28509-28518.	1.5	45
31	Rapid Formation and Macroscopic Selfâ€Assembly of Liquidâ€Crystalline, Highâ€Mobility, Semiconducting Thienothiophene. Advanced Materials Interfaces, 2018, 5, 1700875.	1.9	41
32	Anisotropic charge transport in highly oriented films of semiconducting polymer prepared by ribbon-shaped floating film. Applied Physics Letters, 2018, 112, .	1.5	40
33	Solutionâ€Processed Air‣table Copper Bismuth Iodide for Photovoltaics. ChemSusChem, 2018, 11, 2930-2935.	3.6	39
34	Transparent conductive oxide layer-less dye-sensitized solar cells consisting of floating electrode with gradient TiOx blocking layer. Applied Physics Letters, 2009, 94, .	1.5	38
35	Lead Selenide Colloidal Quantum Dot Solar Cells Achieving High Open-Circuit Voltage with One-Step Deposition Strategy. Journal of Physical Chemistry Letters, 2018, 9, 3598-3603.	2.1	38
36	Improvement of Photovoltaic Performance of Colloidal Quantum Dot Solar Cells Using Organic Small Molecule as Hole-Selective Layer. Journal of Physical Chemistry Letters, 2017, 8, 2163-2169.	2.1	35

#	Article	IF	CITATIONS
37	Controlling Factors for Orientation of Conjugated Polymer Films in Dynamic Floating-Film Transfer Method. Journal of Nanoscience and Nanotechnology, 2017, 17, 1915-1922.	0.9	34
38	Performance Enhancement of Mesoporous TiO ₂ -Based Perovskite Solar Cells by SbI ₃ Interfacial Modification Layer. ACS Applied Materials & Interfaces, 2018, 10, 29630-29637.	4.0	32
39	Dependence of ITO oated Flexible Substrates in the Performance and Bending Durability of Perovskite Solar Cells. Advanced Engineering Materials, 2019, 21, 1900288.	1.6	32
40	Ligand-dependent exciton dynamics and photovoltaic properties of PbS quantum dot heterojunction solar cells. Physical Chemistry Chemical Physics, 2017, 19, 6358-6367.	1.3	31
41	Allâ€Inorganic CsPb _{1â^'<i>x</i>} Ge _{<i>x</i>} I ₂ Br Perovskite with Enhanced Phase Stability and Photovoltaic Performance. Angewandte Chemie, 2018, 130, 12927-12931.	1.6	31
42	Architecture of the Interface between the Perovskite and Holeâ€Transport Layers in Perovskite Solar Cells. ChemSusChem, 2016, 9, 2634-2639.	3.6	27
43	Electronic structures of two types of TiO ₂ electrodes: inverse opal and nanoparticulate cases. RSC Advances, 2015, 5, 49623-49632.	1.7	26
44	New Tin(II) Fluoride Derivative as a Precursor for Enhancing the Efficiency of Inverted Planar Tin/Lead Perovskite Solar Cells. Journal of Physical Chemistry C, 2018, 122, 27284-27291.	1.5	26
45	Structured crystallization for efficient all-inorganic perovskite solar cells with high phase stability. Journal of Materials Chemistry A, 2019, 7, 20390-20397.	5.2	25
46	Recombination Suppression in PbS Quantum Dot Heterojunction Solar Cells by Energy-Level Alignment in the Quantum Dot Active Layers. ACS Applied Materials & Interfaces, 2018, 10, 26142-26152.	4.0	24
47	Enhanced Device Performance with Passivation of the TiO ₂ Surface Using a Carboxylic Acid Fullerene Monolayer for a SnPb Perovskite Solar Cell with a Normal Planar Structure. ACS Applied Materials & Interfaces, 2020, 12, 17776-17782.	4.0	24
48	Investigation of the minimum driving force for dye regeneration utilizing model squaraine dyes for dye-sensitized solar cells. Journal of Materials Chemistry A, 2017, 5, 22672-22682.	5.2	21
49	Anomalous Dielectric Behavior of a Pb/Sn Perovskite: Effect of Trapped Charges on Complex Photoconductivity. ACS Photonics, 2018, 5, 3189-3197.	3.2	21
50	Interface Passivation Effects on the Photovoltaic Performance of Quantum Dot Sensitized Inverse Opal TiO2 Solar Cells. Nanomaterials, 2018, 8, 460.	1.9	20
51	Combined theoretical and experimental approaches for development of squaraine dyes with small energy barrier for electron injection. Solar Energy Materials and Solar Cells, 2017, 159, 625-632.	3.0	18
52	Electrophoretic deposition onto an insulator for thin film preparation toward electronic device fabrication. Applied Physics Letters, 2012, 101, .	1.5	17
53	Transparent conductive oxideâ€less back contact dyeâ€sensitized solar cells using cobalt electrolyte. Progress in Photovoltaics: Research and Applications, 2015, 23, 1100-1109.	4.4	17
54	Rapid Synthesis of Dâ€A′â€Ï€â€A Dyes through a Oneâ€Pot Threeâ€Component Suzuki–Miyaura Couplin Evaluation of their Photovoltaic Properties for Use in Dye‧ensitized Solar Cells. Chemistry - A European Journal, 2016, 22, 2507-2514.	g and an 1.7	17

#	Article	IF	CITATIONS
55	First principles analysis of oxygen vacancy formation and migration in Sr ₂ BMoO ₆ (BA= Mg, Co, Ni). RSC Advances, 2016, 6, 31968-31975.	1.7	15
56	Oxygen vacancy formation and migration in double perovskite Sr ₂ CrMoO ₆ : a first-principles study. RSC Advances, 2016, 6, 43034-43040.	1.7	13
57	Mechanisms of charge accumulation in the dark operation of perovskite solar cells. Physical Chemistry Chemical Physics, 2016, 18, 14970-14975.	1.3	11
58	Concentration gradient-controlled growth of large-grain CH ₃ NH ₃ PbI ₃ films and enhanced photovoltaic performance of solar cells under ambient conditions. CrystEngComm, 2016, 18, 9243-9251.	1.3	11
59	Role of device architecture and AlOX interlayer in organic Schottky diodes and their interpretation by analytical modeling. Journal of Applied Physics, 2019, 126, .	1.1	11
60	Effect of TiO2 Crystal Orientation on the Adsorption of CdSe Quantum Dots for Photosensitization Studied by the Photoacoustic and Photoelectron Yield Methods. Journal of Physical Chemistry C, 2014, 118, 16680-16687.	1.5	10
61	Efficient near infrared fluorescence detection of elastase enzyme using peptide-bound unsymmetrical squaraine dye. Bioorganic and Medicinal Chemistry Letters, 2017, 27, 4024-4029.	1.0	10
62	Effect of Varying Alkyl Chain Length on Thermal Decomposition Temperature of Zinc(II) Xanthates and its Impact on Curing of Epoxy Resin. Zeitschrift Fur Anorganische Und Allgemeine Chemie, 2016, 642, 134-139.	0.6	9
63	Efficient Surface Passivation and Electron Transport Enable Low Temperature-Processed Inverted Perovskite Solar Cells with Efficiency over 20%. ACS Sustainable Chemistry and Engineering, 2020, 8, 8848-8856.	3.2	9
64	Transparent conductive oxideâ€less threeâ€dimensional cylindrical dyeâ€sensitized solar cell fabricated with flexible metal mesh electrode. Progress in Photovoltaics: Research and Applications, 2013, 21, 517-524.	4.4	8
65	Investigation of metal xanthates as latent curing catalysts for epoxy resin via formation of in-situ metal sulfides. Inorganica Chimica Acta, 2015, 435, 292-298.	1.2	7
66	Transparent conductive oxide-less dye-sensitized solar cells (TCO-less DSSC) with titanium nitride compact layer on back contact Ti metal mesh. Journal of Applied Electrochemistry, 2016, 46, 551-557.	1.5	7
67	Dependences of the Optical Absorption, Ground State Energy Level, and Interfacial Electron Transfer Dynamics on the Size of CdSe Quantum Dots Adsorbed on the (001), (110), and (111) Surfaces of Single Crystal Rutile TiO ₂ . Journal of Physical Chemistry C, 2017, 121, 25390-25401.	1.5	6
68	In Situ Fabrication of Integrated Electrode of Perovskite Solar Cells. Chemistry Letters, 2017, 46, 1687-1690.	0.7	6
69	Pb-free Sn Perovskite Solar Cells Doped with Samarium Iodide. Chemistry Letters, 2019, 48, 836-839.	0.7	6
70	Gallium(iii) xanthate as a novel thermal latent curing agent for an epoxy resin composite. RSC Advances, 2014, 4, 24658-24661.	1.7	5
71	Fabrication and characterization of coil type transparent conductive oxide-less cylindrical dye-sensitized solar cells. RSC Advances, 2014, 4, 22959-22963.	1.7	5
72	Relationship between diffusion of Co ³⁺ /Co ²⁺ redox species in nanopores of porous titania stained with dye molecules, dye molecular structures, and photovoltaic performances. RSC Advances, 2015, 5, 83725-83731.	1.7	5

#	Article	IF	CITATIONS
73	Synthesis and Optoelectrical Characterization of Novel Squaraine Dyes Derived from Benzothiophene and Benzofuran. ACS Omega, 2018, 3, 13919-13927.	1.6	5
74	The Effect of Transparent Conductive Oxide Substrate on the Efficiency of SnGe-perovskite Solar Cells. Journal of Photopolymer Science and Technology = [Fotoporima Konwakai Shi], 2019, 32, 597-602.	0.1	5
75	Hot-injection and ultrasonic irradiation syntheses of Cs2SnI6 quantum dot using Sn long-chain amino-complex. Journal of Nanoparticle Research, 2020, 22, 1.	0.8	5
76	Nonisothermal curing kinetics of epoxy resin composite utilizing Ga (III) xanthate as a latent catalyst. Journal of Applied Polymer Science, 2015, 132, .	1.3	4
77	Single-step fabrication of all-solid dye-sensitized solar cells using solution-processable precursor. Physica Status Solidi (A) Applications and Materials Science, 2013, 210, 1846-1850.	0.8	3
78	Crystal Growth, Exponential Optical Absorption Edge, and Ground State Energy Level of PbS Quantum Dots Adsorbed on the (001), (110), and (111) Surfaces of Rutile-TiO ₂ . Journal of Physical Chemistry C, 2018, 122, 13590-13599.	1.5	3
79	Anisotropic Crystal Growth, Optical Absorption, and Ground-State Energy Level of CdSe Quantum Dots Adsorbed on the (001) and (102) Surfaces of Anatase-TiO ₂ : Quantum Dot-Sensitization System. Journal of Physical Chemistry C, 2018, 122, 29200-29209.	1.5	3
80	Stability Improvement of Perovskite Solar Cells by Adding Sbâ€Xanthate to Precursor Solution. Physica Status Solidi (A) Applications and Materials Science, 2020, 217, 2000144.	0.8	3
81	Spun-on carbon antireflective layer with etch resistance for deep and vacuum ultraviolet lithography processes. Journal of Vacuum Science & Technology an Official Journal of the American Vacuum Society B, Microelectronics Processing and Phenomena, 2001, 19, 2385.	1.6	2
82	The Application of Ti Precursor Solutions to Dye-Sensitized Solar Cells. Electrochemistry, 2011, 79, 807-809.	0.6	1
83	Direction to High Efficiency-dye-sensitized Solar Cells. IEEJ Transactions on Fundamentals and Materials, 2008, 128, 573-576.	0.2	1
84	Fabrication of Ion-Paths for Ionic Liquid Type Quasi-Solid Dye Sensitized Solar Cell. Materials Research Society Symposia Proceedings, 2006, 965, 1.	0.1	0
85	Multiple electron injection from dyes to titania layer for high efficiency-dye-sensitized solar cells. , 2011, , .		0
86	Transparent conductive oxide-less back contact dye-sensitized solar cells using Zinc porphyrin dye employing cobalt complex redox shuttle. , 2014, , .		0
87	Introduction of "spike-like" conduction band of TiO2 compact layer for perovskite solar cells. , 0, , .		0
88	Prospects and Challenges with Dye-Sensitized Solar Cells utilizing Far-red Sensitive Dyes and Cobalt Complex Redox Electrolyte. , 0, , .		0